ACADEMIC PRESS

Available online at www.sciencedirect.com

SCIENCE DIRECT®

Journal of Solid State Chemistry 175 (2003) 13–19

JOURNAL OF SOLID STATE CHEMISTRY

http://elsevier.com/locate/jssc

Hydrothermal synthesis of germanium vanadate layered compounds

T. Whitfield,[a] X. Wang,[a] L.-M. Zheng,[b] and A.J. Jacobson[a,*]

[a] *Department of Chemistry, University of Houston, Houston, TX 77204, USA*
[b] *State Key Laboratory of Coordination Chemistry, Coordination Chemistry Institute, Nanjing University, Nanjing 210093, People's Republic of China*

Received 10 September 2002; received in revised form 10 January 2003; accepted 16 January 2003

Abstract

Two novel vanadium oxide–germanium oxide layered compounds $(C_6H_{18}N_2)Ge_2V_4O_{12}(OH)_2 \cdot 2H_2O$ **1** and $CsGeV_2O_6(OH)$ **2**, have been obtained via hydrothermal synthesis from GeO_2, $VOSO_4$ and 1,4-diaminocyclohexane (**1**) or CsOH (**2**). The structure of **1** was determined from single-crystal X-ray data: **1**, monoclinic, $C2/c$, $a = 22.065(3)$ Å, $b = 6.4848(9)$ Å, $c = 14.756(2)$ Å, $\beta = 103.7(1)^\circ$, $V = 2051.67(5)$ Å^3, $Z = 4$. The average structure for compound **2** was determined in a monoclinic subcell, $P2_1/a$, $a = 14.827(5)$ Å, $b = 6.499(2)$ Å, $c = 15.634(5)$ Å, $\beta = 92.1(1)^\circ$, $V = 1505.6(2)$ Å^3, $Z = 8$. The ordered superstructure of **2** has not yet been completely determined. Both structures contain layers built from V_2O_6 chains of edge-shared $V(IV)O_5$ square pyramids that are interconnected by $GeO_3(OH)$ tetrahedra. The interlamellar space is occupied by 1,4-diaminocyclohexane cations and water in **1** and Cs^+ ions in **2**. The magnetic properties of **1** indicate antiferromagnetic coupling between the V(IV) atoms in the chains.

Keywords: Germanium; Vanadium; Oxide; Hydrothermal synthesis; Layered compound

1. Introduction

Layered oxides containing V(IV) or V(V) ions in square pyramidal (VO_5) coordination connected by tetrahedral building units (XO_4 where X= P, As, V) form a large class of compounds. The VO_5 units are isolated in the compounds $VOPO_4 \cdot 2H_2O$ [1], $VOAsO_4 \cdot 3H_2O$ [1], $(NH_4)_2V(V_{2-x}P_x)O_8$ [2–4], and BaV_3O_8 [5] whereas in $VO(HPO_4) \cdot 1/2H_2O$ [6] and $VO(VO_4) \cdot 1/2C_3N_2H_{12}$ [7] V_2O_8 dimers occur. In the pure vanadate phases, increasing the ratio of VO_5 square pyramidal to VO_4 tetrahedral building units leads to structures containing chains of edge-shared pyramids connected by isolated tetrahedra into layers and eventually to compounds with V_2O_5-type pyramidal sheets as reported recently for $V_{18}O_{45}(N_2C_6H_{14})_6$ [8]. The compound $[N(CH_3)_4]_5V_{18}O_{46}$ is an interesting example [9] that is close to the end of the series with $[VO_5]/[VO_4] = 5$.

Of particular relevance to the present work are the compounds with $[VO_5]/[VO_4] = 2$ with the layer structure shown in Fig. 1 for $(C_6H_{14}N_2)V_6O_{14} \cdot H_2O$ [10,11]. Similar compounds include, $N(CH_3)_4V_3O_7$ [12], $(en)_2MV_6O_{14}$ (M = Cu, Zn, Ni), [13,14], $(NH_3CH_3)V_3O_7$, [15], and $[N(CH_3)_4][Co(H_2O)_4 \cdot V_{12}O_{28}]$ [16]. Each layer with the composition V_3O_7 contains a V_2O_6 ribbon of *cis* edge-shared $V(IV)_2O_8$ dimers that are connected together by $V(V)O_4$ tetrahedra. The adjacent ribbons can be connected with different orientations of the dimers and the layers are corrugated or flat depending on the interlayer cations. The relationships between the structures of these compounds have been previously discussed [16,17].

We have recently reported examples of vanadium silicates, niobium silicates, and germanates with open-framework and microporous structures [18–21]. In contrast, our studies of the syntheses of vanadium germanates have resulted so far in a series of cluster anions [22] and the novel vanadium (IV)-germanium oxide layered compounds $(C_6H_{18}N_2)GeV_2O_6(OH) \cdot 2H_2O$ **1** and $CsGeV_2O_6(OH)$ **2** described in this work. The compounds were synthesized under mild hydrothermal conditions and their structures are closely related to those of the compounds with layers of composition V_3O_7 but with $GeO_3(OH)^{3-}$ units replacing VO_4^{3-} tetrahedra.

2. Experimental

2.1. Methods

Reactants used in the synthesis of **1** and **2** were reagent grade and were used as purchased from Aldrich

---

[*] Corresponding author. Fax: +1-713-743-2787.
E-mail address: ajjacob@uh.edu (A.J. Jacobson).

doi:10.1016/S0022-4596(03)00080-X

and Fluka Chemicals. Single-crystal X-ray diffraction was performed with a Siemens SMART platform diffractometer with a 1 K CCD detector with Mo$K\alpha$ radiation. A hemisphere of data was collected using a narrow frame method with scan widths of $0.30°\omega$ with an exposure time of 36 s frame^{-1} for **1** and 35 s frame^{-1} for **2**. All measurements were taken at 293(2) K. The structures were solved by direct methods and refined using SHELXTL [23]. Powder X-ray diffraction data were obtained using a Scintag XDS 2000 diffractometer and Cu$K\alpha$ radiation. Infrared spectra were measured with a Galaxy FTIR 5000 spectrometer using the KBr pellet method. Thermogravimetric measurements were made in nitrogen at a heating rate of 5°C min^{-1} on a TGA V5.1A Dupont 2100. The magnetic susceptibility of **1** was measured on a polycrystalline sample from 2 to 300 K in a magnetic field of 5 kG with a SQUID magnetometer. Diamagnetic corrections were estimated from Pascal's constants.

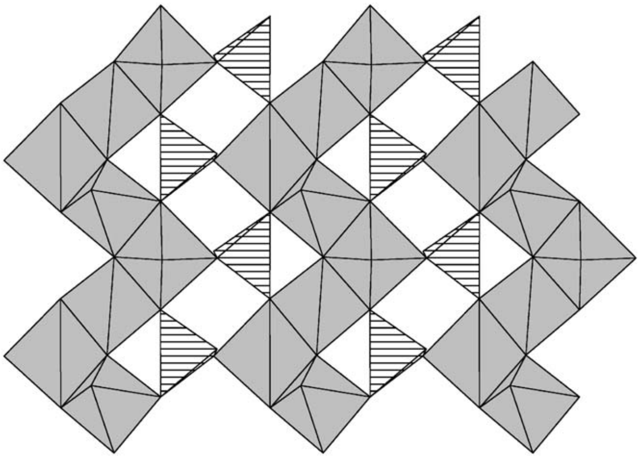

Fig. 1. The structure of the V_3O_7 layer found in $(C_6H_{14}N_2)V_6O_{14}\cdot H_2O$. The VO_5 square pyramids are shaded and the VO_4 tetrahedra are hatched.

2.2. *Synthesis*

2.2.1. *$(C_6H_{18}N_2)Ge_2V_4O_{12}(OH)_2\cdot 2H_2O$* **1**

Compound **1** was formed by the addition of GeO_2 (0.1164 g, 1.1 mmol), $VOSO_4\cdot 4H_2O$ (0.2089 g, 0.9 mmol), 1,4-diaminocyclohexane (1.824 g, 16 mmol), HF (0.29 mL 48% aqueous solution), and H_2O (2.16 mL) into a 23 mL Teflon liner that was placed into a stainless-steel Parr autoclave. The autoclave was heated at 170°C for 7 days. The initial and final pHs were 10 and 9.5, respectively. The product was filtered and washed with deionized water. The resulting washed product was a single phase of green needle crystals in radial clusters (Fig. 2) in an approximate yield of 88% (based on V). IR (KBr cm^{-1}): 3380m, 3095m, 2950m, 1606s, 1519s, 1398w, 1245w, 1141w, 1000s, 970s, 867s, 819s, 763s, 715s, 638s, 588s, 522m.

2.2.2. *$CsGeV_2O_6(OH)$* **2**

Compound **2** was synthesized from a mixture of 4.24M CsOH (1.18 mL, 6 mmol), GeO_2 (0.3138 g, 3 mmol), and 1 M $VOSO_4$ (2 mL, 2 mmol). The mixture was heated in a Teflon-lined stainless-steel Parr autoclave at 240°C for 2 days. The reaction was cooled to room temperature and was then filtered and washed with deionized water. The final pH was 12. After washing, single-phase green hexagonal plate crystals in radial clusters were observed (Fig. 2). IR (KBr cm^{-1}): 3353s, 1635.35w, 993s, 956s, 875s, 823s, 764s, 650s, 592s, 518s, 420w.

3. Results

3.1. *Structure description*

3.1.1. *$(C_6H_{18}N_2)Ge_2V_4O_{12}(OH)_2\cdot 2H_2O$* **1**

Compound **1** crystallizes in the monoclinic space group C2/c (Tables 1–3, Fig. 3). The two inequivalent

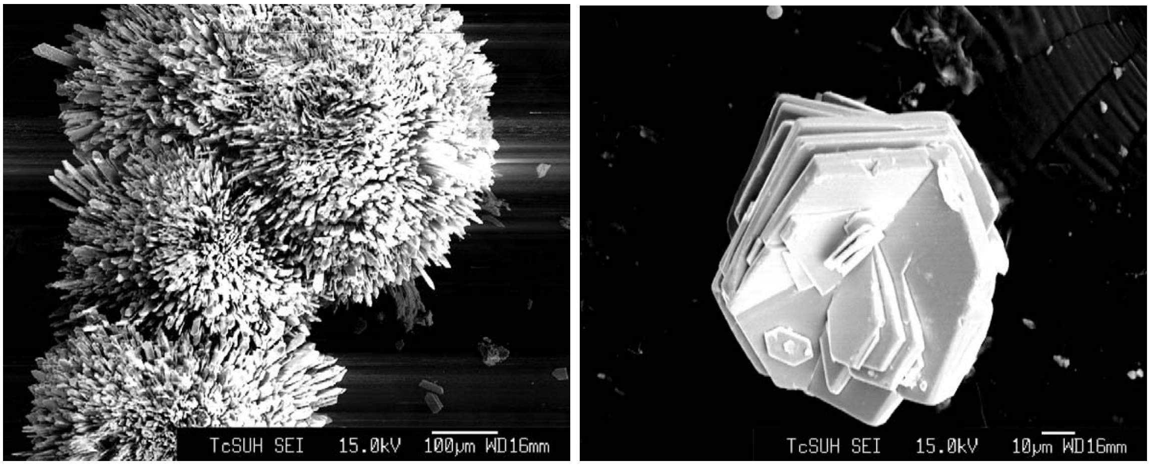

Fig. 2. Scanning electron micrographs of crystals of **1** (left) and **2** (right).

Table 1
Crystallographic data for **1** and **2**

	1	**2**
Formula sum	$C_6H_{22}Ge_2N_2O_{16}V_4$	$HCsGeO_7V_2$
Formula weight	727.2	420.4
Crystal system	Monoclinic	Monoclinic
Space group	$C2/c$ (no. 15)	$P2_1/m$ (no. 4)[a]
Unit-cell dimensions	$a = 22.065(3)$ Å $b = 6.4848(9)$ Å $c = 14.756(2)$ Å $\beta = 103.66(1)^\circ$	$a = 14.827(5)$ Å $b = 6.499(2)$ Å $c = 15.634(5)$ Å $\beta = 92.1(1)^\circ$
Cell volume	2051.7(5) $Å^3$	1505.6(8) $Å^3$
Z	4	8
Density, calculated	2.354 g/cm^3	3.709 g/cm^3
Absorption coefficient	4.718 mm^{-1}	11.152 mm^{-1}
$F(000)$	1424	380[a]
Crystal size (mm)	$0.20 \times 0.03 \times 0.01$	$0.11 \times 0.07 \times 0.03$
Theta range for data collection	1.90–28.42°	2.61–28.42°
Reflections collected	6063	1737[a]
Independent reflections (R_{int})	2381 (0.1028)	596 (0.0645)[a]
Absorption correction	Sadabs	Sadabs
T_{min}/T_{max} ratio	0.8274	0.5003
Data/parameters	2381/139	596/53[a]
Goodness-of-fit on F^2	0.819	1.253[a]
R indices($I > 2\sigma(I)$): $R(F)$, $R_w(F^2)$	0.0449, 0.0608	0.1375, 0.3475[a]
R indices(all data): $R(F)$, $R_w(F^2)$	0.1353, 0.0732	0.1421, 0.3505[a]
Extinction coefficient	0.00022(6)	0.004(6)[a]
Largest diffraction peak and hole	0.622 and −0.785 $eÅ^{-3}$	2.806 and −2.423 $eÅ^{-3}$[a]

$R = \sum(|F_o| - |F_c|)/\sum|F_o|$ and $R_W = (\sum w(|F_o| - |F_c|)^2/\sum wF_o^2)^{1/2}$.
[a] Substructure with $a_{sub} = a/2$, $b_{sub} = b$, $c_{sub} = c/2$.

V(1) and V(2) atoms have square pyramidal coordination with four oxygen atoms in the base and a vanadyl oxygen in the axial position. The V–O bond lengths correspond to those typically observed in V^{4+} O_5 square pyramids. In the $V(1)O_5$ pyramid, the V(1)–O (1,2,3,7) distances in the pyramid base are in the range of 1.918(4)–2.000(5) Å and the apical distance V(1)–O (6) is 1.577(4) Å (Table 3). Similarly, in the $V(2)O_5$ the V (2)–O(1,2,3) distances are in the range 1.921(5)–1.973(5) Å and the V(2)–O(5) distance is 1.609(4) Å. (Table 2). Bond valence calculations confirmed the tetravalence of the vanadium atoms in the layers (V(1) = 4.16, V(2) = 4.18 v.u.) [24]. The $V^{4+}O_5$ square pyramids share edges to form vanadium oxide chains along b (Fig. 4). Each V_2O_5 chain consists of pairs of square pyramids whose terminal vanadyl oxygen atoms are oriented on opposite sides of the chain relative to adjacent pairs of square pyramids. The $V(2)O_5$ share edges with $V(1)O_5$ pyramids. A $V(1)O_5$ pyramid from one dimer shares a *cis* edge with the $V(2)O_5$ pyramids from a second dimer to form the chain.

The germanium atom is bonded to three oxygen atoms and a hydroxyl group. The germanium oxygen

Table 2
Atomic coordinates ($\times 10^4$) and isotropic displacement parameters ($Å^2 \times 10^3$) for **1**

	x	y	z	U_{eq}
Ge(1)	2792(1)	32(1)	716(1)	14(1)
V(1)	3171(1)	−5005(2)	1408(1)	14(1)
V(2)	2767(1)	−7815(2)	2775(1)	13(1)
O(1)	2791(2)	−2210(6)	1392(3)	15(1)
O(2)	2866(2)	−4923(7)	2567(2)	13(1)
O(3)	2932(2)	2049(7)	1525(3)	19(1)
O(4)	3454(2)	−14(8)	263(2)	20(1)
O(5)	3390(2)	−8698(6)	3462(3)	22(1)
O(6)	3902(2)	−4757(8)	1682(3)	23(1)
O(7)	2092(2)	286(7)	−79(3)	18(1)
O(8W)	4385(3)	−10830(9)	2665(4)	75(2)
C(1)	210(3)	−8067(11)	−337(4)	26(2)
C(2)	298(3)	−10627(10)	957(5)	31(2)
C(3)	647(3)	−9380(10)	370(4)	22(2)
N(1)	1130(2)	−8065(9)	967(4)	32(2)

Table 3
Hydrogen coordinates ($\times 10^4$) and isotropic displacement parameters ($Å^2 \times 10^3$)

H(1A)	445	−7355	−722	42(7)
H(1B)	20	−7036	−17	42(7)
H(2A)	112	−9701	1330	42(7)
H(2B)	589	−11 518	1377	42(7)
H(3)	856	−10 347	33	42(7)
H(4A)	1301	−7254	609	42(7)
H(4B)	1423	−8859	1316	42(7)
H(4C)	955	−7291	1334	42(7)
H(51)	3389	−795	−229	42(7)
H(61)	4453	−10 274	3284	42(7)
H(62)	4333	−10 459	2128	42(7)

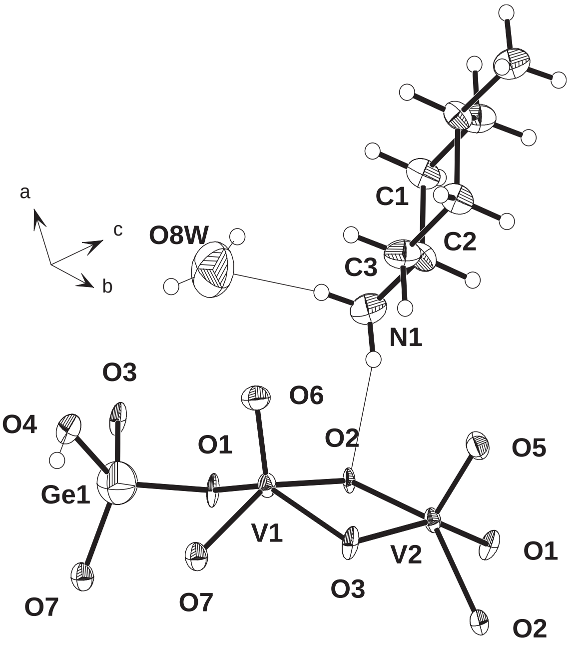

Fig. 3. Part of the structure of **1** showing the atom-labeling scheme. Thin lines indicate hydrogen bonds.

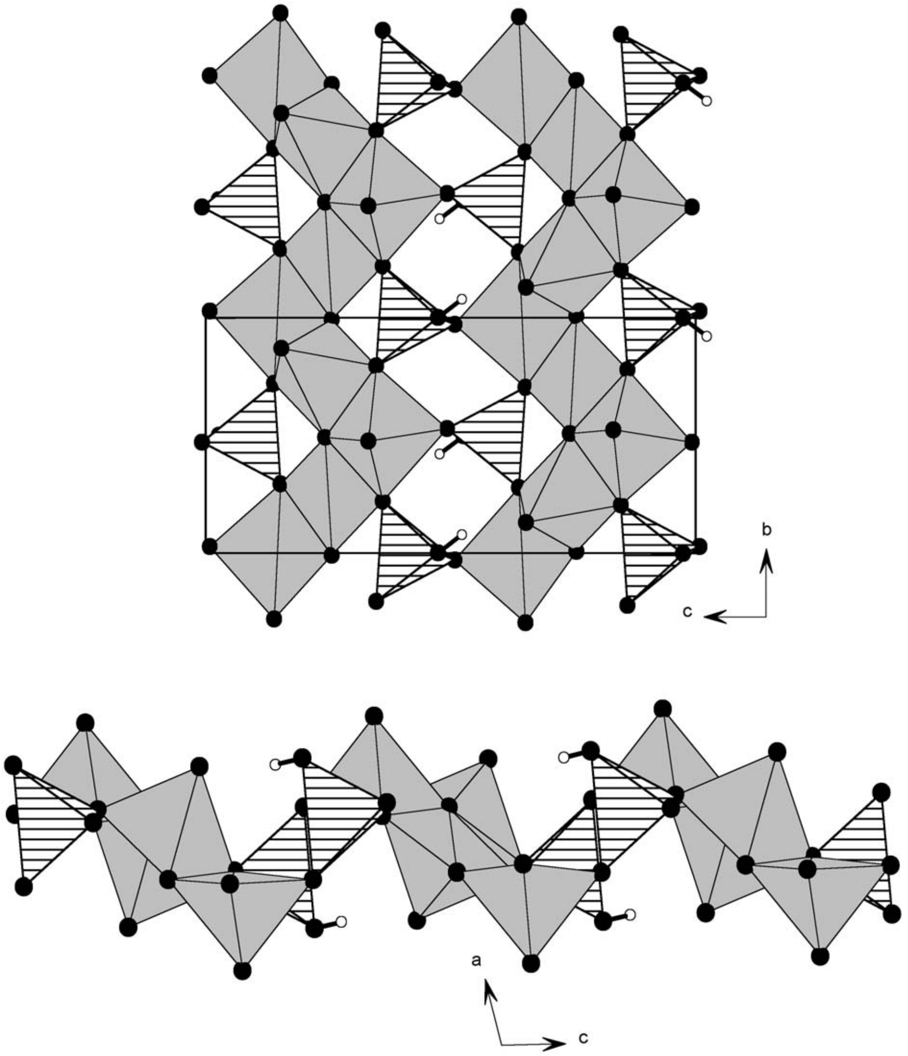

Fig. 4. Polyhedral representation of the layer structure of **1** perpendicular (top) and parallel (bottom) to the layers. The VO_5 square pyramids are shaded and the $GeO_3(OH)$ tetrahedra are white, the black spheres represent oxygen atoms.

bond lengths are all within the normal range, 1.713(4)–1.764(4) Å (Table 4). The $GeO_3(OH)$ tetrahedra are corner shared with the vanadium pyramids, connecting the vanadium oxide chains into layers (Fig. 4). The hydroxyl groups of the germanium tetrahedra are alternately oriented on opposite sides of the layer. The interlayer space is occupied by protonated 1,4-diamino-cylcohexane and water molecules. The structure contains a well-defined network of hydrogen bonds as shown in Fig. 5. The hydrogen bonds are of three distinct types. Intra-layer hydrogen bonds are formed between the germanium hydroxyl group and the vanadyl oxygen atom O(5). The ammonium groups of 1,4-diammoniumcyclohexane are oriented toward the oxide layers and interconnect the layers by forming hydrogen bonds with oxygen atoms O(2) and O(4). The interlayer water molecules ($O_w(8)$) are also hydrogen bonded to the ammonium groups. The hydrogen bond lengths and the O–H···O angles are summarized in Table 5.

3.1.2. $CsGeV_2O_6(OH)$ 2

Compound **2** is structurally related to **1**. Single-crystal diffraction data show a monoclinic superstructure unit cell with $a = 14.827(5)$ Å, $b = 6.499(2)$ Å, $c = 15.634(5)$ Å, $\beta = 92.1(1)^\circ$, space group $P2_1/a$. The reflections with $h = 2n+1$ or $l = 2n+1$ are very weak and efforts to solve the superstructure were not successful. A disordered structure model was solved in the subcell $a_{\mathrm{sub}} = a/2$, $b_{\mathrm{sub}} = b$, $c_{\mathrm{sub}} = c/2$ and space group $P2_1/m$ but with low precision. Nevertheless, the data are sufficient to show that as in compound **1**, the V and Ge atoms in **2** have square pyramidal and tetrahedral coordination, respectively and that the germanium vanadate layer in **2** is closely similar to the

Table 4
Selected bond distances and angles (Å, °) for **1**

Ge1–O1	1.763(4)	N1–H4C	0.891(6)
Ge1–O3	1.748(4)	N1–H4B	0.889(5)
Ge1–O4	1.744(5)	N1–H4A	0.890(6)
Ge1–O7	1.713(4)	N1–C3	1.482(8)
V2–O2$^{\mathrm{i}}$	1.934(5)	C3–H3	0.981(7)
V2–O1$^{\mathrm{i}}$	1.974(5)	C3–C2	1.521(10)
V2–O2	1.921(5)	C3–C1	1.506(8)
V2–O3$^{\mathrm{ii}}$	1.965(5)	C2–H2B	0.971(6)
V2–O5	1.608(4)	C2–H2A	0.969(7)
V1–O3$^{\mathrm{ii}}$	2.000(5)	C2–C1iv	1.525(9)
V1–O6	1.576(4)	C1–H1A	0.972(7)
V1–O2	1.981(4)	C1–H1B	0.969(7)
V1–O1	1.995(4)	C1–C3	1.506(8)
V1–O7$^{\mathrm{iii}}$	1.918(5)	C3–N1	1.482(8)
O4–Ge1	1.744(5)	H4B–N1	0.889(5)
O8W–H61	0.960(6)	H4A–N1	0.890(6)
O8W–H62	0.810(6)		
O3$^{\mathrm{ii}}$–V1–O7$^{\mathrm{iii}}$	88.6(2)	O2$^{\mathrm{i}}$–V2–O1$^{\mathrm{i}}$	77.6(2)
O3$^{\mathrm{ii}}$–V1–O6	110.5(2)	O2$^{\mathrm{i}}$–V2–O5	111.7(2)
V2$^{\mathrm{v}}$–O3–V1$^{\mathrm{v}}$	98.6(2)	O2$^{\mathrm{i}}$–V2–O3$^{\mathrm{ii}}$	90.3(2)
V2–O2–V1	100.7(2)	O3$^{\mathrm{ii}}$–V2–O5	104.8(2)
O2–V1–O1	76.0(2)	O4–Ge1–O7	116.1(2)
O2–V1–O6	108.2(2)	O4–Ge1–O1	108.4(2)
O7$^{\mathrm{iii}}$–V1–O1	92.8(2)	O4–Ge1–O3	104.2(2)
O7$^{\mathrm{iii}}$–V1–O6	108.4(2)	O3–Ge1–O1	104.7(2)
O2–V1–O3$^{\mathrm{ii}}$	78.5(2)	O3–Ge1–O7	112.4(2)
O1–V1–O6	108.2(2)	O7–Ge1–O4	116.1(2)
O2–V2–O3$^{\mathrm{ii}}$	80.8(2)	O7–Ge1–O1	110.2(2)
O2–V2–O5	109.6(2)	N1–C3–C1	109.8(5)
O2–V2–O1$^{\mathrm{i}}$	90.9(2)	N1–C3–C2	110.9(5)
O1$^{\mathrm{i}}$–V2–O5	104.1(2)	H62–O8W–H61	140.7(7)

Symmetry codes: (i) $0.5-x, -0.5+y, 0.5-z$; (ii) $x, -1+y, z$; (iii) $0.5-x, -0.5-y, -z$; (iv) $-x, -2-y, -z$; (v) $x, 1+y, z$.

layer in **1**. In the substructure model of **2** the V(2)O_5 pyramids are randomly disordered between two orientations with oppositely directed apical oxygen corners. In the superstructure, ordered germanium vanadate layers similar to those of **1** are most likely present. The interlayer distance is much smaller in **2** than in **1** due to the smaller size of Cs^+ compared to protonated 1,4-diaminocylcohexane.

3.2. Thermogravimetric analysis

The thermal stability of compound 1 was measured in air with a heating rate of 1°C per minute up to 800°C. Below 100°C, a small weight loss due to surface water was observed followed by the loss of two molecules of water which was complete by 250°C. Beginning at ~200°C, a single weight loss was observed that corresponded to the oxidation of 1,4-diammoniumcylcohexane cations and the loss of water by condensation of the terminal hydroxyl groups coordinated to the germanium atoms. The organic and hydroxyl groups were completely removed by 500°C. At higher temperatures oxidation of V(IV) to V(V) was observed and the final weight at 800°C corresponded closely to the overall composition $GeO_2 \cdot 2VO_{2.5}$.

3.3. Magnetic properties

The temperature dependent molar magnetic susceptibility of **1** in the range 300–2 K is shown in Fig. 6. The $\chi_M T$ value at 300 K is 0.62 $cm^3\,K\,mol^{-1}$, much less than that expected for four isolated $S=\frac{1}{2}$ spins (1.22 $cm^3\,K\,mol^{-1}$ for $g=1.8$). On cooling from room temperature, the $\chi_M T$ decreases continuously and approaches to zero below 50 K, indicating an antiferromagnetic interaction between the magnetic centers with a ground state $S=0$. The antiferromagnetic interaction is also evident by the maximum appearing in the χ_M versus T curve at about 220 K. A further increase below 40 K is due to the presence of paramagnetic impurities.

The structure of **1** contains V/Ge/O layers in which the chains of edge-shared oxovanadium square pyramids are separated by the diamagnetic GeO_4^{4-} groups. Within the chain, the terminal oxo-groups of the neighboring vanadium ions are arranged either *cis* or *trans* [25]. As the unpaired electron in the oxovanadium (IV) complexes usually resides in the d_{xy} orbital with the oxo-group oriented along the z-axis, a direct interaction and/or a superexchange coupling can be present between the magnetic centers [25,26]. Therefore, a rather strong antiferromagnetic interaction is expected when the V···V distance is short and the dihedral angle between the two VO_5 basal planes is close to 0°. In **1**, magnetic exchange may occur between V(1) and V(2) (J_1), V(1) and V(2A) (J_2), or V(2) and V(2A) (J_3) atoms (Scheme 1).

When these three coupling constants are comparable, spin frustration is anticipated because of the triangular arrangement of the magnetic centers. The V(1)···V(2A) (2.989 Å) and V(1)···V(2) (3.006 Å) distances are short compared with the V(2)···V(2A) (3.479 Å) distance. By neglecting the antiferromagnetic interaction between V(2) and V(2A) which is expected to be the weakest, the susceptibility data can be treated with isotropic chain models-either equally spaced or alternating with spin $S=\frac{1}{2}$ [26]. Attempts to fit the data with such models were however, unsuccessful. Assuming that the coupling constant J_2 (= J) between square pyramids in the same (*cis*) orientation is much stronger than J_1 (*trans*) as observed previously [28], the situation can be further simplified as a magnetic dimer system. The susceptibility data were analyzed by the Bleaney–Bowers expression for isotropic dimers of $S=\frac{1}{2}$ ions based on the Heisenberg Hamiltonian $H=-JS_A\cdot S_B$ [27].

$$\chi' = 4Ng^2\beta^2/kT[3+\exp(-J/kT)],$$

$$\chi_M = \chi'/(1-zJ'X')(1-\rho)+\rho Ng^2\beta^2/kT+N_\alpha,$$

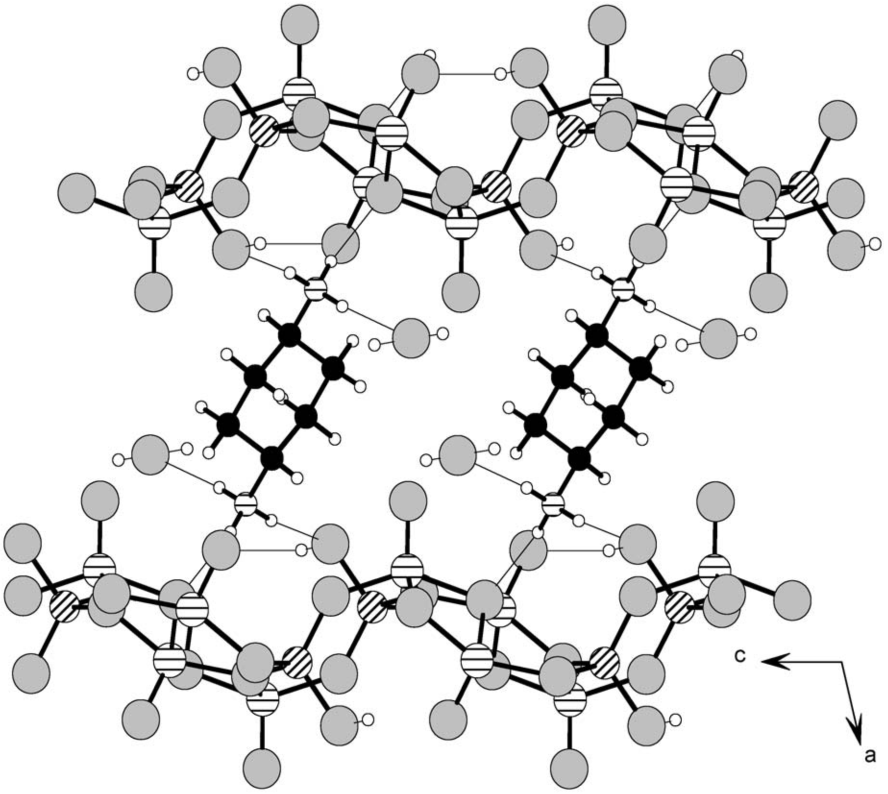

Fig. 5. A view parallel to the layer in **1** showing the arrangement of the piperazine cations and water molecules in the interlamellar space. The hydrogen bonds are shown as thin solid lines. The vanadium, germanium, oxygen, carbon, nitrogen and hydrogen atoms are represented by horizontally hatched, diagonally hatched, gray, black, white, and small horizontally hatched spheres, respectively.

Table 5
Hydrogen bonds in compound **1**

	O–H Å	H···O Å	O–H···O°
O(4)–H···O(5)	0.87(1)	1.960(5)	152.0(2)
N(1)–H···O(2)	0.89(1)	2.106(4)	161.5(4)
N(1)–H···O(4)	0.89(1)	2.107(4)	168.8(4)
N(1)–H···O$_w$(8)	0.89(1)	2.041(7)	171.1(4)

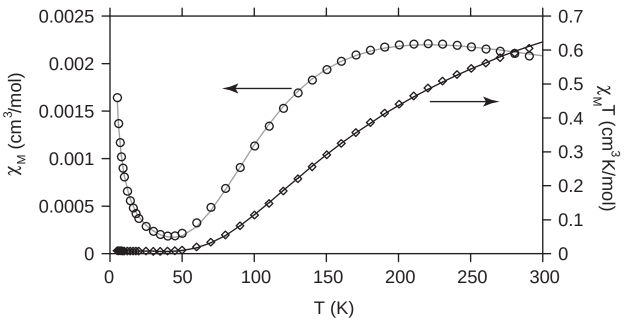

Fig. 6. Magnetic susceptibility data for **1**. Open symbols are the experimental data and the solid lines are the calculated fit.

where zJ' accounts for the inter-dimer interactions, ρ is the molar fraction of mononuclear impurities, and N_α is the sum of the diamagnetic and TIP contributions. A good fit was obtained with $g = 1.66$, $J = -244.9\,\text{cm}^{-1}$, $\rho = 0.0081$, $zJ' = -29.9\,\text{cm}^{-1}$, $N_\alpha = -38.4 \times 10^{-6}\,\text{cm}^3\,\text{mol}^{-1}$. When g is fixed to be 1.8, the theoretical fitting, shown as a solid line in Fig. 6, leads to parameters $J = -250.8\,\text{cm}^{-1}$, $\rho = 0.0069$, $zJ' = -83.1\,\text{cm}^{-1}$, $N_\alpha = -38.4 \times 10^{-6}\,\text{cm}^3\,\text{mol}^{-1}$. The resulting J value of compound **1** are comparable to those observed in other oxovanadium dimer complexes [26]. Magnetic data have been reported previously for the $(\text{en})_2\text{MV}_6\text{O}_{14}$ (M = Cu,

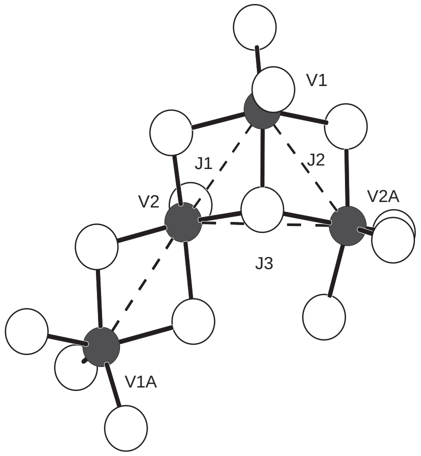

Scheme 1.

Zn) members of the layered [V_3O_7] compound series. [13] In these compounds the V(IV, d^1)O_5 square pyramidal chains are connected by V(V, d^0)O_4 tetrahedra. The magnetic data indicate that as observed in **1**, the V(IV) spins become antiferromagnetically coupled below room temperature [13].

4. Conclusion

Two novel vanadium oxide–germanium oxide layered compounds, $(C_6H_{18}N_2)Ge_2V_4O_{12}(OH)_2 \cdot 2H_2O$ **1** and $CsGeV_2O_6(OH)$ **2**, have been obtained via hydrothermal synthesis from GeO_2, $VOSO_4$ and 1,4-diaminocyclohexane (**1**) or CsOH (**2**). The structure of **1,** determined from single-crystal X-ray data contains layers built from V_2O_6 chains of edge-shared V(IV)O_5 square pyramids that are interconnected by $GeO_3(OH)$ tetrahedra. The interlamellar space is occupied by 1,4-diaminocyclohexane cations that are hydrogen bonded to the layers and to interlayer water molecules. The magnetic properties of **1** were modeled as antiferromagnetic coupled V(IV) dimers weakly coupled to each other along the chain. Compound **2** has the same arrangement of VO_5 square pyramids and GeO_3OH tetrahedra in the layer. An average and disordered structure was determined for a subcell of the true structure. The superstructure has not yet been completely determined.

Acknowledgments

This work was supported by the National Science Foundation under Grant DMR-0120463 and by the Robert A. Welch Foundation. The work made use of MRSEC Shared Experimental Facilities supported by the National Science Foundation under Award Number DMR-9632667.

References

[1] J.W. Johnson, A.J. Jacobson, J.F. Brody, S.M. Rich, Inorg. Chem. 21 (1982) 3820.
[2] S. Boudin, A. Grandin, P. Labbe, B. Raveau, Acta. Crystallogr. C 52 (1996) 2668.
[3] C. Ninclaus, R. Retoux, D. Riou, G. Férey, J. Solid State Chem. 122 (1996) 139.
[4] L. Liu, X. Wang, R. Bontchev, K. Ross, A.J. Jacobson, J. Mater. Chem. 9 (1999) 1585.
[5] Y. Oka, T. Yao, N. Yamamoto, J. Solid State Chem. 117 (1995) 407.
[6] J.W. Johnson, C.C. Johnston, A.J. Jacobson, J.F. Brody, J. Am. Chem. Soc. 106 (1984) 8123.
[7] D. Riou, G. Férey, J. Solid State Chem. 120 (1995) 137.
[8] M. Sicard, A. Maignan, D. Riou, Solid State Sci. 4 (2002) 285.
[9] B. Koene, N.J. Taylor, L.F. Nazar, Angew. Chem. Int. Ed. Engl. 111 (1999) 234.
[10] L.F. Nazar, B.E. Koene, J.F. Britten, Chem. Mater. 8 (1996) 327.
[11] Y. Zhang, R.C. Haushalter, A. Clearfield, Chem. Commun. (1996) 1055.
[12] T.G. Chirayil, E.A. Boylan, M. Mamak, P.Y. Zavalij, M.S. Whittingham, Chem. Commun. (1997) 33.
[13] Y. Zhang, J.R.D. DeBord, C.J. O'Connor, R.C. Haushalter, A. Clearfield, J. Zubieta, Angew. Chem. Int. Ed. Engl. 35 (1996) 989.
[14] P.Y. Zavalij, F. Zhang, M.S. Whittingham, Acta Crystallogr. B 55 (1999) 953.
[15] R. Chen, P.Y. Zavalij, M.S. Whittingham, J.E. Greedan, N.P. Raju, M. Bieringer, J. Mater. Chem. 9 (1999) 93.
[16] X. Wang, L. Lumei, A.J. Jacobson, K. Ross, J. Mater. Chem. 9 (1999) 859.
[17] P.Y. Zavalij, M.S. Whittingham, Acta Crystallogr. B 55 (1999) 627.
[18] X. Wang, L. Liu, A.J. Jacobson, Angew. Chem. Int. Ed. Engl. 40 (2001) 2174.
[19] R.J. Francis, A.J. Jacobson, Angew. Chem. Int. Ed. Engl. 40 (2001) 2879.
[20] R.J. Francis, A.J. Jacobson, Chem. Mater. 13 (2001) 4676.
[21] X. Wang, L. Liu, A.J. Jacobson, J. Am. Chem. Soc. 124 (2002) 7812.
[22] X. Wang, X.L. Liu, G. Zhang, A.J. Jacobson, Chem. Commun. (2001) 2472.
[23] G.M. Sheldrick, SHELXTL, Program for Refinement of Crystal Structure, Siemens Analytical X-ray Instruments Inc., Madison, WI, 1994.
[24] N.E. Brese, M. O'Keeffe, Acta. Crystallogr. B 47 (1991) 192.
[25] W. Plass, Angew. Chem. Int. Ed. Engl. 35 (1996) 627.
[26] W. Plass, Z. Anorg. Allg. Chem. 623 (1997) 1290, and references therein.
[27] O. Kahn, Molecular Magnetism, VCH Publishers, Inc., New York, 1993.
[28] J. Do, L.-M. Zheng, R.P. Bontchev, A.J. Jacobson, Solid State Sci. 3 (2000) 343.